Induction of apoptosis in B16-BL6 melanoma cells following exposure to electromagnetic fields modelled after intercellular calcium waves

Benjamin D. Rain, Adam D. Plourde-Kelly, Robert M. Lafrenie, & Blake T. Dotta*

Behavioural Neuroscience & Biology Programs
School of Natural Science
Laurentian University, Sudbury, Ontario, P3E2C6, Canada

Corresponding Author:
Dr. Blake Dotta
Behavioural Neuroscience
Laurentian University
Sudbury, ON, Canada
P3E 2C6
Tel:1-705-675-4824
bx_dotta@laurentian.ca

Running head: Melanoma Apoptosis: EMF and Calcium Wave Influence

Abbreviations

Ca2+: Calcium
EMF: Electromagnetic fields
ICW: Intercellular calcium waves
VGCC: voltage-gated calcium channels
B16-BL6: B16-BL6 Mouse melanoma cells
HEK 293: Human embryonic kidney cells
A + A: Antibiotic and antimycotic cell culture solution
CO2: Carbon dioxide
BAY K8644: BAY K8644 L-type calcium channel activator
uT: micro tesla
Ω: Ohm
Cm: centimeter
Mm: millimeter
Ml: milliliter
μg: microgram
ANOVA: analysis of variance
IBM SPSS: International Business Machines Statistical Processing Software
EB: ethidium bromide dye
AO: acridine orange dye
Hz: hertz
SEM: Standard error of the mean
Act: Activator (BAY K8644 L-type calcium channel activator)

Abstract

Exposure to time-varying electromagnetic fields (EMF) have the capacity to influence biological systems. Our results demonstrate that exposure to time-varying EMF modeled after the physiological firing frequency of intercellular calcium waves can inhibit proliferation and induce apoptosis in malignant cells. Single exposure of B16-BL6 cells to a Ca2+ EMF for 40 minutes reduced the number of viable cells by 50.3%. Cell imaging with acridine orange and ethidium bromide dye revealed substantial cellular apoptosis, pre-apoptotic cells, nuclear fragmentation, and large spacing between cells in the Ca2+ EMF condition when compared to the control condition. The ability for Ca2+ EMF to influence the proliferation and survival of malignant cells suggests that exposure to specific EMF may function as a potential anti-cancer therapy.

2

1. Introduction

Biological systems are continuously encompassed by Electromagnetic fields (EMF) [1]. These EMFs can be static or dynamic. A dynamic EMF is a propagating field of force that displays temporal variations in intensity and direction. Over the past century, much effort has gone into generating artificial EMFs that emulate those that occur naturally [2, 3]. Modeling the intensities and temporal signatures of the natural EMF environment into an artificial field allows for the generation of indistinguishable patterns from those produced by biological systems [4, 5]. Thus manufactured EMFs have the potential to elicit naturally occurring focal and global interactions [4]. Complex EMFs, such as those designed to imitate physiologically-relevant processes, have demonstrated the ability to modulate the function of the specific process they were modeled after. For example, we have previously demonstrated that the frequency-modulated "Thomas" patterned EMF alters cell membrane activity [6]. Additionally, rodents exposed to the Thomas field for 180 min/day demonstrated impaired memory performance and an increased analgesic response [6-8].

Calcium signaling is a form of cellular communication essential for the development, conservation, and propagation of many biological systems [9]. This process allows for neighboring cells to communicate with one another and for the entire system to communicate with its environment [10]. Among the most pronounced forms of calcium signaling are intercellular calcium waves [11]. Intercellular calcium waves (ICW) are naturally occurring physiological processes that commence with an increase in Ca2+ within a cell that propagates to nearby cells in a wave-like manner [12]. The process appears to provide the necessary level of communication for a single cell to communicate with its cohort, thereby establishing a multicellular response [12].

Modification of intracellular calcium concentration [Ca2+] influences the duration and intensity of the Ca2+ wave [11]. Changes in intracellular Ca2+ occurs via the opening of voltage and ligand gated Ca2+ channels that allow for a flux of Ca2+ across the plasma membrane, or the liberation of Ca2+ from internal reserves such as the endoplasmic reticulum (ER) [11]. Alternatively, the Ca2+ increase may also occur as a result of Ca2+ in the extracellular environment. Voltage-gated calcium channels (VGCC) are Ca2+ permeable ion channels located on the plasma membrane of a cell [13]. There are three principal categories of VGCC: low-voltage activated (T-type), high/intermediate voltage activated (P/R-type) and high-voltage activated (L-type) [14, 15]. The primary role of VGCCs is to transduce electrical changes from the plasma membrane into an intracellular response [14]. The influx of Ca2+ through VGCC is central to the development, proliferation, and apoptosis of a cell; hence proper functioning of these channels is required for cellular homeostasis [15-17].

Two different cell lines were employed in this study, B16-Bl6 and HEK293. The B16-BL6 cells are derived from a mouse melanoma tumor, while the HEK293 are derived from human embryonic kidney cells. B16-BL6 cells serve as an adequate model for Ca2+ waves due to the high prevalence of T-type voltage-gated Ca2+ channels while the HEK293 cells express very low levels of T-type channels [6, 18, 19]. Activation of T-type channels occurs following a small membrane depolarization and demonstrates a unique

3

pattern of activation/inactivation present at low voltage (18). Previous biomolecular studies have demonstrated the ability for specific patterned EMFs to influence T-type calcium channels associated with the inhibition of malignant cell proliferation [4]. Furthermore, T-type voltage-gated Ca2+ channels have been shown as a mechanism for malignant cell signaling by which intercellular communication occurs as a traveling wave of Ca2+ [20]. Because of this previous research, both a malignant (B16BL6) and non-malignant (HEK293) cell line were chosen.

Due to the aforementioned research it was of interest to determine if an EMF modeled after the physiological firing frequency of an ICW could influence Ca2+ signaling in the absence of pharmacological or mechanical intervention. It was our hypothesis that an EMF patterned after ICW would decrease the number of viable B16-BL6 cells and promote apoptosis. We hypothesized, based on previous research, that this effect would occur predominantly in the B16-BL6 cells, due to the high amount of T-type voltage-gated Ca2+ channels.

2. Materials and Methods

2.1 Cell Maintenance

B16-BL6 and HEK293T cells were obtained from the American Type Culture Collection (Manassas, VA) and cultured on 100 mm medium adherence culture plates in DMEM/high glucose media (Hyclone, Fisher, Mississauga, ON) supplemented with 10% fetal bovine serum, and 1% antibiotic and antimycotic (A + A). Cells were subcultured 1:5 biweekly and mainained in a culture incubator at 37°C, 5% CO2 and 100% humiei5y For experiments, the cells were harvested and approximately 200,000 cells were added to a 60 mm medium-adherence experimental plate and cultured overnight before treatments..

For some experiments, the cells were treated with 5 µM BAY K8644, a VDCC activator, immediately before exposure to the sham or EMF conditions. Experimental plates were then placed in the incubator at 37°C, 5% CO2 for 48 hours.

2.2 EMF Exposure

On the day of EMF exposure, experimental plates were gathered from the incubator and treated according to their labeled treatment condition. Control (sham-treated) plates were placed in a dark Styrofoam box at 22⁰C for the duration of the 40 min exposure time. The box was kept in a separate room more than 10 feet away from the EMF exposure apparatus. Experimental plates (Ca-EMF) or Sine-EMF field conditions were placed in the dark, in the center of a field generator at 22⁰C. The EMF was applied for 40 minutes. Following exposure, cells were removed from the field generator and returned to the incubator at 37°C, 5% CO2 for 48 hours.

2.3 Field Design and Application

The EMF employed in this study (Figure 1) was modeled after the physiological activation pattern of calcium waves in murine cells located in the longitudinal layer of the cecum and colon. The pattern of EMF was modeled after a study conducted by Hennig et al.,[21] in which intra- and intercellular calcium wave activity was recorded. From these recordings, we then plotted a graph displaying the relative amplitudes of calcium wave activity. The resulting pattern of this graph was used to design an EMF with identical amplitude, frequency, and temporal characteristics to a naturally occurring calcium wave. The EMF was generated using a digital-to analog device created by Stanley Koren [22]. Its important to note that our EMF design was modeled after the physiological firing pattern of calcium waves and was not designed to be a perfect replication. In this case, we are concerned with modeling the appropriate pattern rather than matching the exact amplitudes. The resulting amplitudes of the Ca2+ EMF are proportional to the original pattern, with the maximum intensity emitted by the EMF being 4uT. The pattern completed a full cycle in approximately 5 seconds. This pattern was generated by a computer, which was connected to an EMF-generating device, inducing an electric current. The generating device was a 30 Ω Helmholtz coil comprised of a 39 cm x 39 cm box wrapped by 305 m of 30 American Wire Guage insulated copper wire. All EMFs employed in this study were emitted at an intensity of 1 micro tesla which coincides with the intensities of numerous biomolecular pathways. Cell plates were placed in the middle of the generating device and left in the dark for the entire 40-minute duration of the field exposure. The passing of current horizontally through the copper wire generated a corresponding magnetic field of approximately 4 µT in the vertical direction which then passes inside the generating device on to the cell plates.

2.4 Cell Counting

Experimental plates were removed from the incubator 48 hours following treatment. Cells were harvested and counted [23] using a standard Neubauer ruled 1 mm² hemocytometer and inverted phase-contrast microscope. The number of viable and non-viable cells present in one 0.25 x 0.20 mm square were counted in duplicate measures and the number of cells/ml was calculated

2.5 Cell Imaging

Experimental plates were removed from the incubator 48 hours following treatment. All cells were treated with 5 µg/ml acridine orange and 5 µg/ml ethidium bromide for 15 minutes prior to imaging. Images were captured using a Zeiss Axiovert 200 M zoom inverted microscope using the bright field, red, and green channels using the ZEN 3.5 Blue Edition editing software created by Zeiss.

2.6 Statistical Analysis

All data were computed using IBM SPSS statistical analysis software version 28. The data presented for the number of viable cells were computed from raw scores tallied using the hemocytometer counting procedure. Additionally, the data displaying percent viability was calculated using a formula obtained from the Sigma – Aldrich protocol [23]. Levene's test was used to test for homogeneity of variance for both number of

viable cells, and percent viability. A one-way ANOVA was conducted, and an independent samples T-test was performed to compare subsets of those data which were normally distributed. In data that violated the homogeneity of variance assumption, a Kruskal Wallace and Mann Whitney U independent samples test was used to compare data subsets. No outliers were excluded from the statistical analyses.

3. Results

3.1 Reduction of B16-BL6 Viability Following Exposure to Ca2+ EMF

A significant effect was observed between the three treatment conditions (No EMF, Sine EMF, Ca2+ EMF) and the number of viable cells counted [F (2,46) = 5.77, p = 0.006]. An independent samples T-test revealed that cells subjected to the Ca2+ EMF condition had significantly fewer viable cells (50.3%) when compared to the No EMF condition [T (36) = 2.36, p = 0.012] (Fig. 2). Further, cells subjected to the Ca2+ EMF condition displayed significantly fewer viable cells than those in the Sine EMF condition [H (1) = 11.78, p < 0.001] (Fig. 2). Conversely, there was no effect on viable cells, non-viable cells, or total cells when utilizing the HEK293 cell line [F (2,46) = 0.265, p = 0.768] (Figure 3).

3.2 BAY K Calcium Channel Activator Interacts with Ca2+ EMF

To determine the effect of BAY K8644 on the Ca2+ EMF, the data were separated according to the presence or absence of activator (Figure 4). In the B16-BL6 cells that received no calcium activator, there was a significant difference between the Ca2+ EMF and all other treatment conditions (refer to section 3.1). In the cells that received the calcium activator and Ca2+ EMF, there was no significant difference in the number of viable cells [H (2) = 2.838, p = 0.242].

3.3 Effect on Percentage Viability

To determine the influence of each treatment condition on the percentage viability (Fig. 5), raw viability scores were used to calculate the percentage of viable cells using the formula provided in the Sigma – Aldrich hemocytometer protocol [23]. B16-BL6 cells exposed to the Ca2+ EMF condition displayed significantly fewer viable cells when compared to the No EMF condition [H (1) = 9.06, p = 0.003] and the Sine EMF condition [H (1) = 11.02, p< 0.001].

3.4 Cell imaging

Cell imaging of B16-BL6 cells subjected to the Ca2+ EMF revealed substantial nuclear orange – red fluorescence by ethidium bromide (EB), while other cells displayed a strong yellow-green fluorescence in their nuclei by acridine orange (AO) staining (Fig. 6). Additionally, cells under the Ca2+ EMF condition appear more uniformly distributed with less aggregation and greater spacing between cells. Similar results were observed by cells in the BAY k 8644 + Ca2+ EMF condition which displayed a large amount of orange-red, and yellow-green fluorescence in the cells' nuclei; however, the distribution of cells appeared more variable with cells more tightly packed, forming dense clusters.

The intensity of the yellow-green and orange-red (AO/EB) stains was greater in the BAY k 8644 + Ca2+ EMF condition when compared to all other conditions (Fig. 7).

4. Discussion

This is the first known experiment to employ a complex EMF modeled after the physiological firing of ICWs. The results demonstrate that a dynamic, physiologically patterned EMF can inhibit the proliferation of malignant cells and induce cell death. A single exposure of the Ca2+ modeled EMF resulted in a significant decrease in the mean number of viable cells by 50.3%. The proposed mechanism of action for these specific-frequency EMFs involves enhancing the presence of reactive oxygen species, differential activation of cellular signaling cascades, and the induction of a rapid Ca2+ influx, all of which are proposed to decrease cell growth and induce apoptosis [24-26]. Furthermore, work by Stratton, Lange, & Inal., [27] demonstrates that malignant cells exposed to extremely low-frequency EMFs with an energy of 0.3 µT at a consistent frequency of 10Hz, show a compromised plasma membranes allowing for an influx of Ca2+ that subsequently enhances apoptosis.

The Ca2+ EMF is a complex-time varying pattern housing multiple frequencies that are fluctuating as the field is emitted. As demonstrated in the results, cells exposed to the simple 3Hz sine wave showed no alteration in proliferation or cell death. Given these findings, it is proposed that the timing and pattern of the frequencies emitted from the EMF to the cells play a crucial role in the field's efficacy to alter proliferation and induce cell death. Conversely, cells treated with the BAY K8644 activator and exposed to the Ca2+ EMF did not display a significant decrease in their mean number of viable cells compared to the No EMF group and Bay k8644 + No EMF group. The BAY K8644 calcium activator is a voltage-gated L-type calcium channel agonist that increases Ca2+ channel permeability resulting in a brief Ca2+ influx [28]. The kinetics of this activator are different from the traditional, long-lasting action of L-type calcium channels. The addition of BAY K8644 promotes maximal Ca2+ uptake within 10 minutes of administration, leading to a large increase in cytoplasmic Ca2+ concentration, which then declines to resting levels in the following 30 minutes [6, 28, 29]. The ability for BAY K8644 to inhibit the effects of Ca2+ EMF suggests that the efficacy of the field lies in its ability to alter the kinetic properties of L-type and T-type voltage-gated Ca2+ channels. Additionally, the lack of an effect with the HEK293 cells is significant. It demonstrates the specificity of the Ca2+ EMF mechanism. Cancer is a direct result of alterations in the mechanisms attributed to the proliferation and death of a cell [30]. Since Ca2+ signaling is crucial to both processes, the importance of Ca2+ kinetics within and between cells cannot be overemphasized [30, 31]. Intracellular increases in Ca2+ are central to a variety of cellular signaling events such as Ca2+ sparks, oscillations, and waves [12, 32, 33]. The dysregulation of calcium signaling is detrimental to normal cell functioning and is associated with the hallmarks of cancer [34]. The abnormal Ca2+ signaling found in malignant cells occurs through the modification and differential expression of Ca2+ channels and pumps [15, 33]. While the cellular machinery (Ca2+ channels, pumps, and exchangers) is the same in both non-malignant and malignant cells, the latter may express cellular machinery with alternative isoforms, location, activity, and gene mutations associated with cancerous

7

processes [15]. Modification of this machinery alters the intra and intercellular flux of Ca2+ for a given cell as described by the abnormal movement of ions across the plasma membrane [15, 17].

Considering the original Buckner studies [6] and the results from the current study, it is proposed that the mechanism of the Ca2+ EMF acts specifically on T-type voltage-gated calcium channels. Cells exposed to the Ca2+ EMF for a 40-minute duration in the absence of the BAY K8644 activator displayed the full anti-cancer effects. However, cell treated with the BAY K8644activator prior to field exposure did not demonstrate these properties. In accordance with the findings of Buckner et al., [6], we hypothesize the opposing action of the BAY K8644 activator resides in its ability to stimulate a flux of Ca2+ through L-type VGCCs that is necessary for malignant cell survival. Due to the dysregulation in Ca2+ signaling and alteration in cellular machinery associated with cancer, the BAY K8644 activator may function to enhance typical malignant Ca2+ signaling through altered cellular machinery.

Cell imaging using AO/EB staining revealed a substantial amount of orange-red and yellow-green fluorescence in the nuclei of Ca2+ EMF treated cells (Fig. 6 B). As demonstrated by Liu *et al.,* [35], cells displaying orange-red fluorescence in their nuclei are regarded as late apoptotic, whereas those displaying yellow-green fluorescence are considered early apoptotic. It is important to note that complete apoptosis was not observed from these figures however, the stark color contrast among different experimental conditions is indicative of different apoptotic stages. The high prevalence of late and early apoptotic cells observed in the Ca2+ EMF condition is consistent with the findings of Morrone, Gehring, & Nicoletti., [15], whereby inappropriate flow of Ca2+ through T-type calcium channels resulted in anti-proliferative effects and apoptosis in glioma cells. Conversely, images of the Activator + Ca2+ EMF group displayed comparable results under AO/EB staining (Fig. 6 A). A similar number of early and late apoptotic cells were noted, however, with a more intense fluorescence indicative of nuclear condensation. While both groups appeared to have similar degrees of cellular apoptosis, cells in the Ca2+ EMF condition displayed a more uniform distribution with less aggregation and greater spacing between cells. These findings are consistent with the results in figure 3, demonstrating a decrease in the mean number of viable cells for the group exposed to the Ca2+ EMF.

The presence of apoptosis in the absence of an effect for the BAY K8644 + Ca2+ EMF group suggests that there is a temporal component underlying the anti-proliferative, cell death-inducing mechanism of the Ca2+ EMF. The Ca2+ influx through L-type channels associated with BAY K 8644 occurs within 10 min of administration and returns to resting concentrations within 30 min. Since administration of the activator suppressed the effects of Ca2+ EMF, it is proposed that the field functions by increasing T-type Ca2+ channel permeability, allowing for a gradual Ca2+ influx over the 40-minute exposure period. The kinetic action of the BAY K 8644 activator causes a transient Ca2+ increase through L-type channels in the same timeframe the field is active. The competing action of the BAY K 8644 activator may be working to promote normal malignant cell Ca2+ signaling through altered L-type channels while Ca2+ EMF is working to cause irregular, disruptive signalling through T-type channels. We propose that these two competing actions lead to substantial interference whereby the residual effect is negligible.

8

Findings from this study further support the hypothesis that complex-patterned EMFs can influence cells, their cohorts, and entire biological systems. These data demonstrate the ability for a physiologically patterned EMF modeled after the activation frequency of Ca2+ waves to seize proliferation and induce apoptosis in a malignant cell model. We propose that exposure to Ca2+ EMF alters T-type Ca2+ channel permeability allowing for an irregular Ca2+ influx capable of disturbing proliferation and inducing apoptosis of malignant cells. Future studies should investigate the specific mechanisms and timing at which the Ca2+ EMF alters calcium channel permeability. Such information would provide valuable insights into our current observations suggesting that the Ca2+ EMF could act as a potential anti-cancer therapy.

Author Contribution: Conceptualization, BDR, BTD; methodology, BDR, RML and BTD; formal analysis, BDR, BTD; investigation, BDR, ADPK, BTD; resources, RML, BTD; data curation, BDR; writing—original draft preparation, BDR; writing—review and editing, BDR, BTD; supervision, BTD; project administration, RML, BTD

Conflict of Interest: The authors declare no conflicts of interest

Data Accessibility: The data that support the findings of this study are available on request from the corresponding author. The data are not publicly available due to privacy or ethical restrictions

5. References

1 Rouleau, N, and Dotta, BT. (2014) Electromagnetic fields as structure-function zeitgebers in biological systems: environmental orchestrations of morphogenesis and consciousness. Frontiers in Integrative neuroscience 8: 84.

2 Saroka, KS, and Persinger, MA. (2013) Potential production of Hughlings Jackson's "parasitic consciousness" by physiologically-patterned weak transcerebral magnetic fields: QEEG and source localization. Epilepsy & Behavior 28, no. 3: 395-407.

3 Mach, QH, and Persinger, MA. (2009) Behavioral changes with brief exposures to weak magnetic fields patterned to stimulate long-term potentiation. Brain research 1261: 45-53.

4 Buckner, C. (2012) Effects of electromagnetic fields on biological processes are spatial and temporal-dependent. Library and Archives Canada.

5 Dotta, BT, Lafrenie, RM, Karbowski, LM and Persinger, MA. (2014) Photon emission from melanoma cells during brief stimulation by patterned magnetic fields: is the source

coupled to rotational diffusion within the membrane. General Physiology and Biophysics 33: 63-73.

6 Buckner, CA, Buckner, AL, Koren, SA, Persinger, MA and Lafrenie, RM. (2015) Inhibition of cancer cell growth by exposure to a specific time-varying electromagnetic field involves T-type calcium channels. PLoS One 10, no. 4: e0124136.

7 Martin, LJ, Koren, SA and Persinger, MA. (2004) Thermal analgesic effects from weak, complex magnetic fields and pharmacological interactions. Pharmacology Biochemistry and Behavior 78, no. 2: 217-227.

8 Shupak, NM, Prato, FS and Thomas, AW. (2004) Human exposure to a specific pulsed magnetic field: effects on thermal sensory and pain thresholds. Neuroscience letters 363, no. 2 : 157-162.

9 Berridge, MJ, Bootman, MD and Roderick, LH. (2003) Calcium signalling: dynamics, homeostasis and remodelling. Nature reviews Molecular cell biology 4, no. 7 : 517-529.

10 Bootman, MD, Collins, TJ, Peppiatt, CM, Prothero, LS, MacKenzie, L, De Smet, P, Travers, M. "Calcium signalling—an overview. (2001) In Seminars in cell & developmental biology, vol. 12, no. 1, pp. 3-10. Academic Press.

11 Ross, WN. (2012) Understanding calcium waves and sparks in central neurons. Nature Reviews Neuroscience 13, no. 3: 157-168.

12 Leybaert, L, and Sanderson, MJ. (2012) Intercellular Ca2+ waves: mechanisms and function. Physiological reviews 92, no. 3: 1359-1392.

13 Catterall, WA, and Swanson, TM. (2015) Structural basis for pharmacology of voltage-gated sodium and calcium channels. Molecular pharmacology 88, no. 1: 141-150.

14 Catterall, WA. (2011) Voltage-gated calcium channels. Cold Spring Harbor perspectives in biology 3, no. 8: a003947.

15 Morrone, FB, Gehring, MP and Nicoletti, NF. (2016) Calcium channels and associated receptors in malignant brain tumor therapy. Molecular pharmacology 90, no. 3: 403-409.

16 Chen, YF, Chen, YT, Chiu, WT and Shen, MR. (2013) Remodeling of calcium signaling in tumor progression. Journal of biomedical science 20, no. 1 : 1-10.

17 Prevarskaya, N, Skryma, R, and Yaroslav, S. (2013) Targeting Ca2+ transport in cancer: close reality or long perspective?. Expert opinion on therapeutic targets 17, no. 3: 225-241.

18 Ohkubo, T, and Yamazaki, J. (2012) T-type voltage-activated calcium channel Cav3. 1, but not Cav3. 2, is involved in the inhibition of proliferation and apoptosis in MCF-7 human breast cancer cells. International journal of oncology 41, no. 1 : 267-275.

19 Berjukow, S, Döring, F, Froschmayr, M, Grabner, M, Glossmann, H and Hering, S. (1996) Endogenous calcium channels in human embryonic kidney (HEK293) cells. British journal of pharmacology 118, no. 3 : 748-754.

20 Huang, JB, Kindzelskii, AL, Clark, AJ and Petty, HR. (2004) Identification of channels promoting calcium spikes and waves in HT1080 tumor cells: their apparent roles in cell motility and invasion. Cancer research 64, no. 7 : 2482-2489.

21 Hennig, GW, Smith, CB, O'Shea, DM and Smith, TK. (2002) Patterns of intracellular and intercellular Ca2+ waves in the longitudinal muscle layer of the murine large intestine in vitro. The Journal of Physiology 543, no. 1 : 233-253.

22 Buckner, CA, Buckner, AL, Koren, SA, Persinger, MA and Lafrenie, RM. (2018) Exposure to a specific time-varying electromagnetic field inhibits cell proliferation via cAMP and ERK signaling in cancer cells. Bioelectromagnetics 39, no. 3: 217-230.

23 Sigma-Aldrich. Cell Counting Using a Hemocytometer. Millipore Sigma (2022). Retrieved from https://www.sigmaaldrich.com/CA/en/technical-documents/technical-article/cell-culture-and-cell-culture-analysis/mammalian-cell-culture/cell-quantification

24 Wolf, FI, Torsello, A, Tedesco, B, Fasanella, S, Boninsegna, A, D'Ascenzo, M, Grassi, C, Azzena, GB and Cittadini, A. (2005) 50-Hz extremely low frequency electromagnetic fields enhance cell proliferation and DNA damage: possible involvement of a redox mechanism. Biochimica et Biophysica Acta (BBA)-Molecular Cell Research 1743, no. 1-2: 120-129.

25 Simkó, M. (2007) Cell type specific redox status is responsible for diverse electromagnetic field effects. Current medicinal chemistry 14, no. 10 : 1141-1152.

26 Destefanis, M, Viano, M, Leo, C, Gervino, G, Ponzetto, A and Silvagno, F. (2015) Extremely low frequency electromagnetic fields affect proliferation and mitochondrial activity of human cancer cell lines. International Journal of Radiation Biology 91, no. 12 : 964-972.

27 Stratton, D, Lange, S and Inal, JM. (2013) Pulsed extremely low-frequency magnetic fields stimulate microvesicle release from human monocytic leukaemia cells. Biochemical and biophysical research communications 430, no. 2 : 470-475.

28 Sanguinetti, MC, Krafte, DS and Kass, RS. (1986) Voltage-dependent modulation of Ca channel current in heart cells by Bay K8644. The Journal of general physiology 88, no. 3: 369-392.

29 Zahradníková, A, Minarovič, I and Zahradník, I. (2007) Competitive and cooperative effects of Bay K8644 on the L-type calcium channel current inhibition by calcium channel antagonists. Journal of Pharmacology and Experimental Therapeutics 322, no. 2 : 638-645.

30 Capiod, TY, Skryma, SR, and Prevarskaya, N. (2007) Calcium signalling and cancer cell growth. Calcium Signalling and Disease: Molecular Pathology of Calcium : 405-427.

31 Borowiec, AS, Bidaux, G, Pigat, N, Goffin, V, Bernichtein, S and Capiod, T. (2014) Calcium channels, external calcium concentration and cell proliferation. European journal of pharmacology 739 : 19-25.

32 Dupont, G, Combettes, L. Bird, GS and Putney, JW. (2011) Calcium oscillations. Cold Spring Harbor perspectives in biology 3, no. 3: a004226.

33 Monteith, GR, Davis, FM and Roberts-Thomson, SJ. (2012) Calcium channels and pumps in cancer: changes and consequences. Journal of Biological Chemistry 287, no. 38 : 31666-31673.

34 Stewart, TA, Yapa, KT and Monteith, GR. (2015) Altered calcium signaling in cancer cells. Biochimica et Biophysica Acta (BBA)-Biomembranes 1848, no. 10 : 2502-2511.

35 Liu, K, Liu, PC, Liu, R, & Wu, X (2015). Dual AO/EB staining to detect apoptosis in osteosarcoma cells compared with flow cytometry. Medical science monitor basic research, 21, 15.

Figure Legends

Figure 1. Activation pattern of intra and intercellular calcium waves in murine cells located in the longitudinal layer of the cecum and colon, modelled after Hennig et al., [21]

Figure 2 – Mean number of viable B16-BL6 cells by EMF condition, no activator. Data analysis revealed significant differences between the Ca2+ EMF condition and No EMF condition [T (36) = 2.36, *p = 0.012] and the Ca2+ EMF condition and Sine EMF condition [H (1) = 10.931, **p < 0.001]. Statistical analysis conducted using T-test (T) and Kruskal Wallis test (H). Sine EMF n = 8, Control EMF n = 16, Ca2+ EMF n = 10. Error bars represent SEM.

12

Figure 3. Mean number of viable HEK293T cells per EMF exposure condition. Statistical analysis revealed no significant difference in the number of viable cells between exposure conditions. Error bars represent SEM.

Figure 4 – Mean number of viable B16-BL6 cells by EMF condition with activator. Kruskal Wallis test: [H (2) = 2.838, p = 0.242]. Act + No EMF = 6, Act + Sine EMF n = 4, Act + Calcium EMF n = 6. Error bars represent SEM**.**

Figure 5 – Percentage B16-BL6 cell viability by EMF treatment condition. Kruskal Wallis test: [H (1) = 9.06, *p = 0.003] [H (1) = 11.02, **p< 0.001]. No EMF n = 16, Sine EMF n = 8, Ca2+ EMF n = 10, Act + No EMF n = 6, Act + EMF Sine n = 4, Act + EMF (Ca2+) n = 6. Error bars represent SEM.

Figure 6 – B16-BL6 cell imaging with acridine orange and ethidium bromide staining. **A.** BAY k 8644 + Ca2+ EMF, **B.** Ca2+ EMF, **C.** BAY k 8644 + No EMF, **D.** No EMF. Scale bar length = 10μm.

Figure 7 - Cell imaging of EMF treated B16-Bl6 and HEK293T cells stained with acridine orange and ethidium bromide : **A**. B16-BL6 + Ca2+ EMF, **B**. B16-BL6 cells + No EMF **C.** HEK293T + Ca2 EMF, **D.** HEK293T + No EMF. Scale bar length = 10μm.
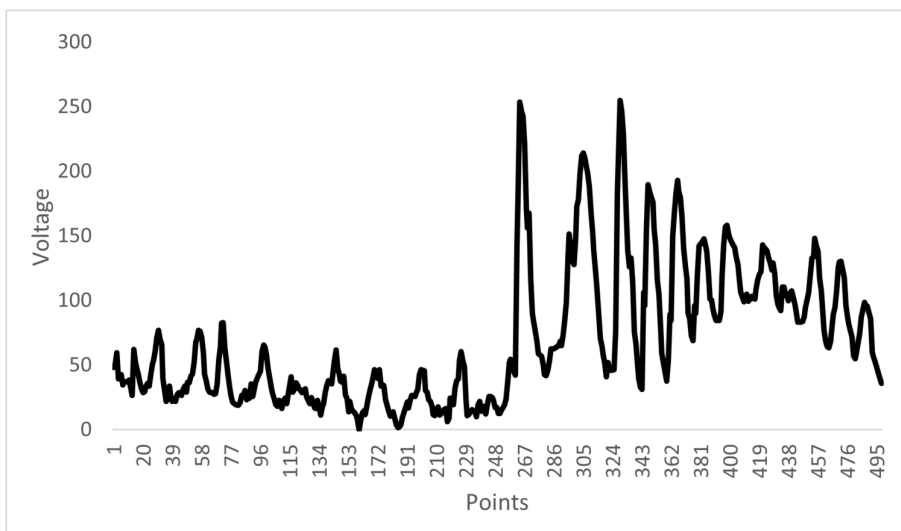
Figure 1.tif

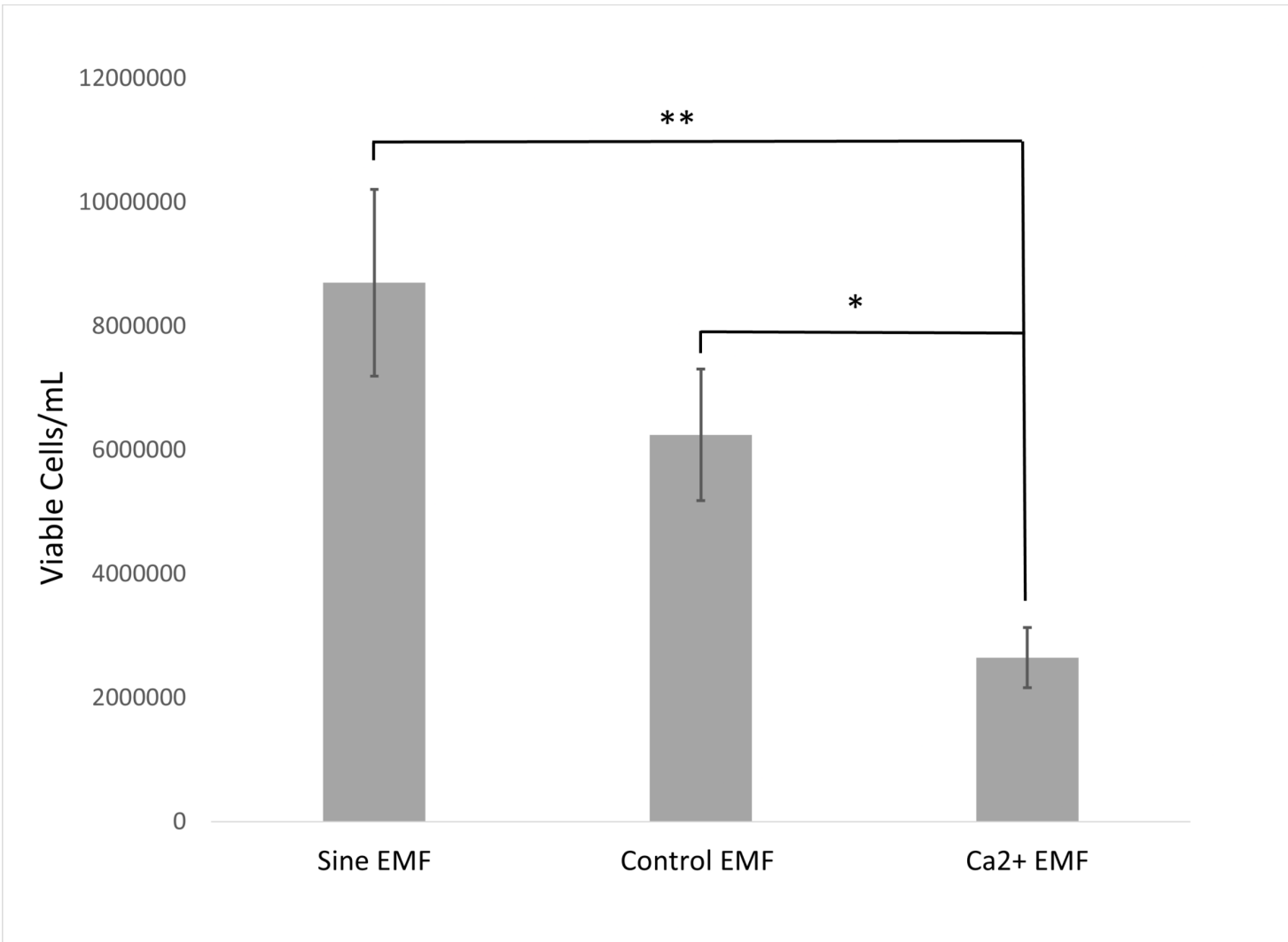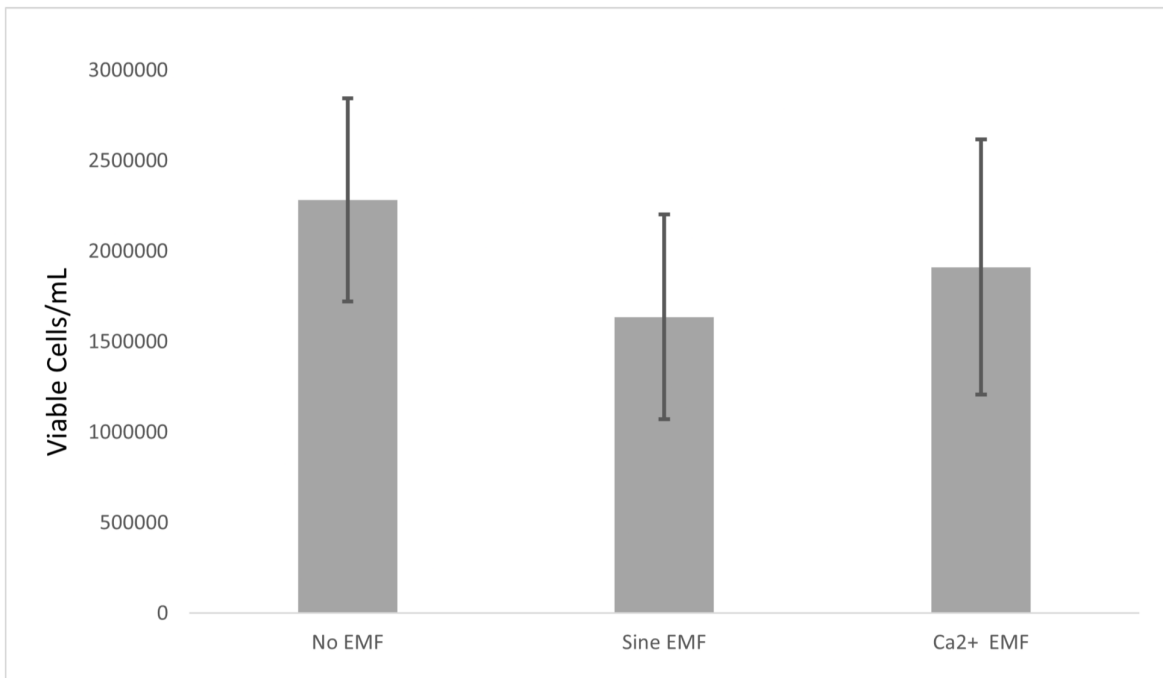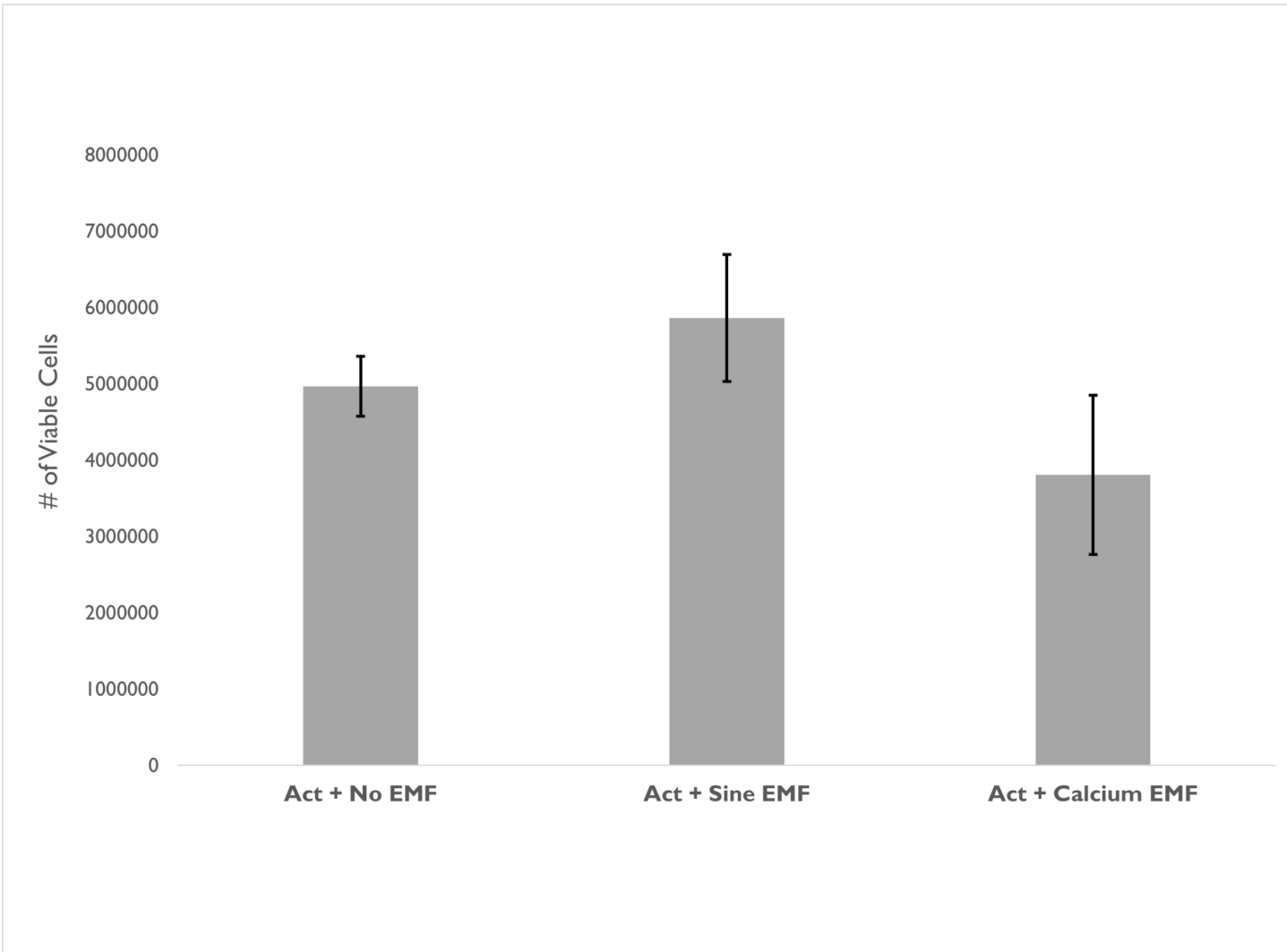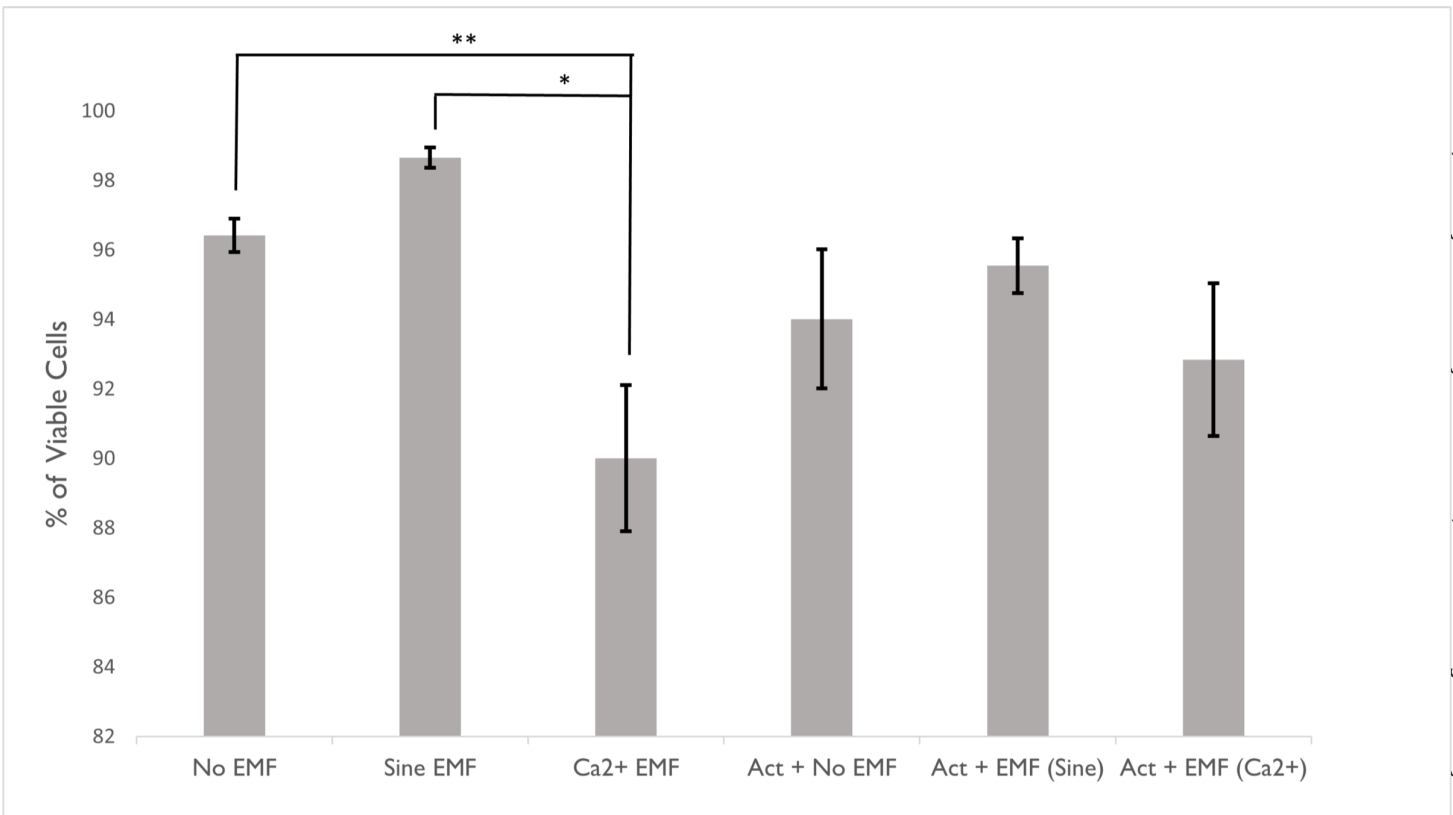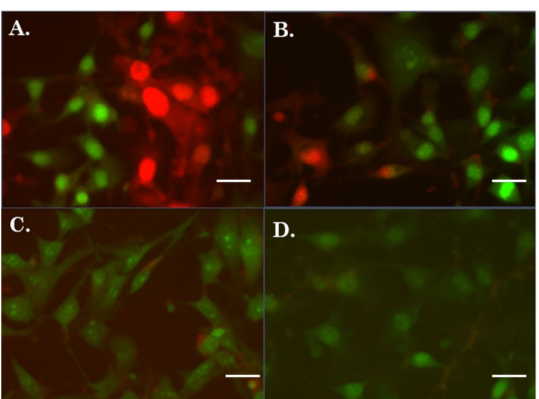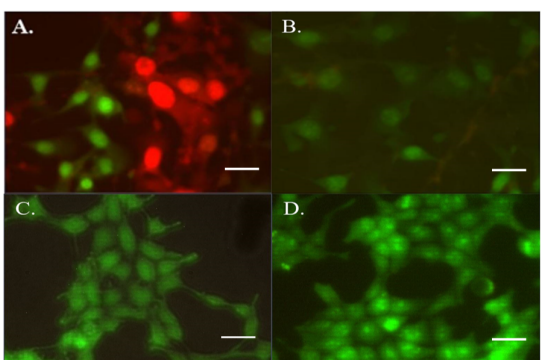Figure 2.0.tif

Figure 3.0.tif

Figure 4.tif

Figure 5.tif

Figure 6.tif

Figure 7.tif